Available online at www.sciencedirect.com

SciVerse ScienceDirect

Journal of the European Ceramic Society 32 (2012) 619–625

www.elsevier.com/locate/jeurceramsoc

Effect of Al_4SiC_4 additive on the densification of β-silicon carbide under vacuum

Jin-Seok Lee [a,*], Young-Soo Ahn [a], Toshiyuki Nishimura [b], Hidehiko Tanaka [b], Sea-Hoon Lee [c]

[a] *Korea Institute of Energy Research, Daejeon 305-343, Republic of Korea*
[b] *National Institute for Materials Science, Tsukuba, Ibaraki 305-0044, Japan*
[c] *Korea Institute of Materials Science, Changwon 641-831, Republic of Korea*

Received 21 November 2010; received in revised form 23 September 2011; accepted 1 October 2011
Available online 22 October 2011

Abstract

The potential of ternary compound (Al_4SiC_4) powders as an effective sintering additive to concurrently achieve SiC densification and grain refinement was evaluated under vacuum. Nearly fully densified SiC ceramic was successfully obtained in the absence of a residual liquid phase at the grain boundaries using low temperature hot pressing at 1700 °C by adding 10 wt% Al_4SiC_4 as an additive. The main mechanism for obtaining SiC densification was analyzed with changing additive contents. A larger amount of additive content was effective in suppressing the grain growth of SiC due to the formation of newly generated carbon by the thermal decomposition of Al_4SiC_4. Regardless of the additive content, sintering temperature and grain size, the fracture mode of the Al_4SiC_4-doped SiC mainly consisted of intragranular fractures due to the high interfacial bonding strength.

Keywords: Al_4SiC_4; SiC; Hot pressing; Sintering; Grain boundaries

1. Introduction

Silicon carbide (SiC) ceramic is a promising candidate for use in applications such as gas turbines, piston engines, and heat exchangers due to its many advantages such as high melting temperature, low density, high strength, and good chemical and oxidation resistances.[1,2] However, SiC is one of the most difficult polycrystalline materials to sinter because of the covalent bonding of SiC. Various approaches have been attempted to lower the sintering temperature of SiC by designing a sintering additive through liquid- or solid-phase sintering mechanisms.[3,4] When oxide additives[4] are added, SiC densification could be easily achieved at low temperatures with accompanying the formation of an amorphous interphase at the grain boundaries. On the other hand, the densification of SiC with non-oxide additives[3,5] frequently occurs by a solid-state diffusion process, which usually requires sintering temperatures higher than 2000 °C.[5] Boron has been shown to be a very efficient additive for the low temperature sintering of SiC, but liquid phases such as borosilicate glass[6] or melts of $Al_8B_4C_7$[7] were reported to form during heating, which may decrease the high temperature properties of the sintered SiC. In addition, B additive can induce significant grain growth of SiC during sintering.[8] The fabrication of a fully dense SiC with a non-oxide additive in the absence of boron is very difficult at temperatures as low as 1700 °C using hot pressing method.

Recently, a ternary compound (Al_4SiC_4) has received strong attention because it shows outstanding oxidation and corrosion resistances due to the formation of dual oxide layers.[9,10] Moreover, in a recent study, the present authors analyzed the thermal decomposition behavior of Al_4SiC_4 powders above 1450 °C by reaction (1).[11]

$$Al_4SiC_4 \rightarrow 4Al_{(g)} + SiC_{(s)} + 3C_{(s)} \quad (1)$$

Al source has been shown to be an effective sintering aid for SiC, and the incorporation of Al into SiC does not strongly affect the SiC grain growth compared to B additive.[12,13] Excess carbon originating from reaction (1) is also useful for removing oxygen impurities and retarding the grain growth of SiC.[14] Therefore, it is believed to be possible to obtain fine grained SiC as a result. The above discussion indicates that there is great potential for

* Corresponding author. Tel.: +82 42 860 3745; fax: +82 42 860 3133.
E-mail address: jslee@kier.re.kr (J.-S. Lee).

0955-2219/$ – see front matter © 2011 Elsevier Ltd. All rights reserved.
doi:10.1016/j.jeurceramsoc.2011.10.003

Table 1
The relative densities and mechanical properties of the SiC compacts sintered by hot pressing under a pressure load of 60 MPa under vacuum at various sintering temperatures and Al_4SiC_4 additive contents.

Sample name	Batch composition [wt%]		Temperature [°C]	Relative density [%]	Hardness [GPa]	Fracture toughness [MPa $m^{1/2}$]
	SiC	Al_4SiC_4				
ASC1	90	10	1600	72.4	–	–
ASC2	90	10	1700	99.4	22.5	4.4 ± 0.5
ASC3	90	10	1800	99.0	23.6	4.3 ± 0.2
ASC4	90	10	1900	99.9	23.3	4.8 ± 0.4
ASC5	95	5	1800	99.2	24.4	4.4 ± 0.3
ASC6	98	2	1800	99.6	23.8	4.4 ± 0.2

Al_4SiC_4 powders as an effective sintering additive for concurrently obtaining SiC densification and grain refinement under vacuum.

In the present work, we investigated the effect of Al_4SiC_4 compound additive on the densification of SiC ceramics in the temperature range of 1600–1900 °C. Also, the effort to verify the dominant mechanism for SiC densification was carried out with various additive contents.

2. Experimental procedure

The synthetic conditions of Al_4SiC_4 were described elsewhere in detail.[11] Commercially available nano β-SiC powders (T-1 grade, Sumitomo Osaka Cement Co., Tokyo, Japan) with a mean particle size of 30 nm containing around 3 wt% free carbon and 0.45 wt% oxygen were mixed with 2, 5, and 10 wt% of the as-synthesized Al_4SiC_4 powder in ethyl alcohol for 24 h using a planetary mill. A SiC ball and jar apparatus was used to minimize contamination during the milling. The slurries were dried at 60 °C for 24 h in a vacuum dryer and then sieved through a 150 μm mesh. The powder mixtures were placed into a carbon mold (10 mm in diameter) and the gap between the mold and the carbon cap was sealed using a BN slurry to minimize vaporization of the metallic gases. Subsequently, the powders were hot-pressed in the range of 1600–1900 °C for 2 h at a heating rate of 50 °C/min under a pressure load of 60 MPa under vacuum ($<7 \times 10^{-3}$ Pa) or in flowing Ar. Table 1 summarizes sintering conditions such as sintering temperatures and Al_4SiC_4 additive contents for various samples. ASC1 indicates SiC compacts with 10 wt% Al_4SiC_4 sintered at 1600 °C, ASC2 at 1700 °C, ASC3 at 1800 °C, and ASC4 at 1900 °C. ASC5 and ASC6 indicate SiC compacts with 5 wt% and 2 wt% Al_4SiC_4 sintered at 1800 °C for 2 h, respectively. In all cases, the consolidated samples were cooled down to room temperature by turning off the power.

The relative densities of the samples with around 10 mm in diameter and 3 mm height were calculated by Archimedes' method based on theoretical densities that are determined using the rule of mixture (SiC: 3.21 g/cm^3, Al_4SiC_4: 3.03 g/cm^3). Phase identification of each product was determined by X-ray diffractometry (XRD, RINT-UltimaIII, Rigaku Co., Tokyo, Japan) using Cu Kα radiation (wavelength of 1.54056 Å). Quantitative measurements of the polytype content in the sintered SiC specimens were simply calculated using the XRD peaks.[15] The sintered samples were polished and plasma-etched in a mixture of CF_4 and 8% O_2. The microstructure of the samples was observed through scanning electron microscopy (SEM, JSM-6700F, JEOL Ltd., Tokyo, Japan). The atomic and structural natures of the grain and grain boundary phases were also examined using high-resolution transmission electron microscopy (HR-TEM, JEM-4000EX, JEOL Ltd., Tokyo, Japan). Chemical compositions of grain and grain boundary phases were analyzed by an energy dispersive X-ray (EDX) spectrometer equipped with a TEM facility. Fracture toughness was evaluated by using the indentation fracture (IF) method, in which five indentations were made with a 49 N load on the polished surface of each sintered sample. The toughness values were calculated using the equation proposed by Anstis et al.[16] and were then averaged. The elastic modulus of every ceramic sample, which was needed to calculate the fracture toughness in the IF method, was measured by the pulse echo method (5072PR, Panametrics Inc., Massachusetts, USA).

3. Results and discussion

3.1. Reaction between SiC and Al_4SiC_4

Fig. 1 shows XRD patterns of Al_4SiC_4 compacts sintered at 1700 and 1800 °C, and SiC compact with 10 wt% Al_4SiC_4 sintered at 1700 °C for 2 h by hot pressing under an applied pressure load of 60 MPa in flowing Ar. For the single-phase Al_4SiC_4 compacts (Fig. 1(a) and (b)), there was no phase change after heat-treatment, which means that Al_4SiC_4 did not decompose during hot pressing at 1800 °C in Ar. In contrast to monolithic Al_4SiC_4, thermal decomposition of Al_4SiC_4 was observed during hot pressing at 1700 °C in Ar when mixed with SiC (Fig. 1(c)). This obviously indicates that SiC induces the decomposition of Al_4SiC_4 accompanying carbon generation in the matrix because carbon could not be formed from SiC decomposition due to the high thermal decomposition temperature of SiC (2830 ± 40 °C).[17]

From a crystallographic perspective, Al_4SiC_4 can be described as an Al_4C_3-type crystal with hexagonal 4H–SiC-type structural units alternatively stacked along the *c*-direction.[18] The decomposition of Al_4SiC_4 originates from breaking the bonds of the Al_4C_3-type unit because the Al–C bonds are considerably weaker than the Si–C bonds in Al_4SiC_4.[18] If Al_4SiC_4 directly contacted SiC during densification, the ternary compound may preferentially decompose according to reaction (1) due to the

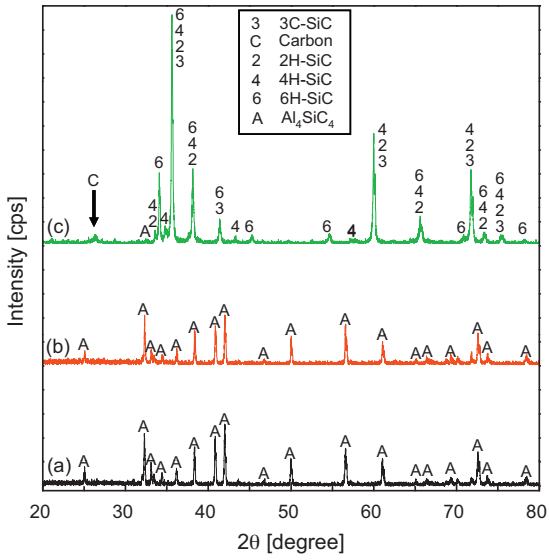

Fig. 1. XRD patterns of single-phase Al_4SiC_4 compacts sintered at (a) 1700 °C, (b) 1800 °C, and (c) SiC compact with 10 wt% Al_4SiC_4 sintered at 1700 °C for 2 h by hot pressing under an applied pressure load of 60 MPa in flowing Ar.

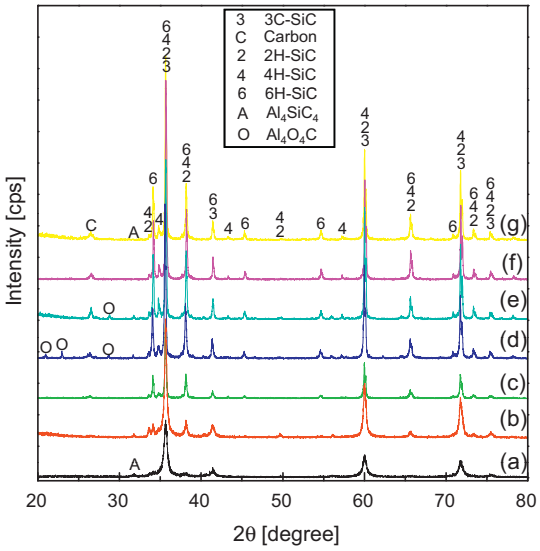

Fig. 2. XRD patterns of (a) a raw mixture of SiC and 10 wt% Al_4SiC_4, (b) ASC1, (c) ASC2, (d) ASC3, (e) ASC4, (f) ASC5, and (g) ASC6.

concentration gradient of Al between the two materials. In this case, the resultant Al resides at SiC grain boundaries or dissolves into the neighboring SiC to form a Al–SiC solid solution. This phenomenon will be discussed in detail using TEM analysis.

During the densification of SiC using Al_4SiC_4 additive, Al is expected to induce the densification of SiC. Accordingly, heat-treatment under vacuum with a lower Al partial pressure should be more adequate to generate Al sources than heat-treatment in flowing Ar. Indeed, we found out the thermal decomposition reaction (reaction (1)) of Al_4SiC_4 above 1450 °C under vacuum and the concentration gradient of Al in Al_4SiC_4–SiC system is believed to promote the Al_4SiC_4 decomposition.[11] Based on the above results, the following sintering tests were performed under vacuum.

3.2. Phase formation and transformation during densification

Fig. 2 shows the XRD patterns of a raw powder mixture of β-SiC and 10 wt% Al_4SiC_4, and dense SiC bodies (ASC1–ASC6). According to the phase identification of a raw mixture (Fig. 2(a)) of β-SiC and Al_4SiC_4 powders milled with a SiC ball and jar, a small amount of α-SiC in the raw mixture was caused by contamination from the SiC ball and jar. All of the sintered specimens consisted of a SiC phase together with residual Al_4SiC_4 and newly generated C. However, carbon peaks were not detected in the raw powder mixture (Fig. 2(a)) and ASC1 because a relatively small amount of carbon was formed by the decomposition of the additive. Compared to the XRD pattern of the raw mixture, all of the sintered SiC bodies show a significant β to α phase transformation. This means that the decomposition of the additive induced SiC phase transformation, in which part of the Al atoms derived from the decomposition of Al_4SiC_4 additive dissolved into the SiC lattice.[7] Pure β-SiC (3C phase) is a metastable phase, and the temperature required to transform into α-SiC (6H phase) was reported to be 1800–1850 °C.[19] AlB_2-carbon additives were reported to lower the transformation temperature to 1800 °C,[20] whereas boron and carbon suppress the behavior.[21] Accordingly, aluminum is believed to significantly lower the transformation temperature. Phase transformation in ASC1 was around 11% without considering the contaminated α-SiC content, but those in ASC2–ASC4 were nearly 100% when 10 wt% additive was used. Compared to the results of Tanaka et al.[20,22] using AlB_2-carbon additives, the onset temperature of phase transformation in this research was about 200 °C lower, presumably due to the absence of boron which suppress the transformation.[20,21] Phase transformations in ASC5 and ASC6 were 93% and 71%, respectively. This clearly indicated that Al_4SiC_4 promotes the phase transformation of SiC.

Al_4O_4C peaks were detected in the SiC compacts with 10 wt% additive sintered above 1800 °C. Oxygen for forming the oxycarbide compound mainly originated from Al_2O_3 on the surface of Al_4SiC_4 (oxygen content of as-prepared powder: 0.83 wt%), because the cases of ASC5 and ASC6 did not show Al_4O_4C phases. The oxygen content of Al_4SiC_4 presumably increased during wet mixing and drying process.

Al_4O_4C seemed to form through reaction with carbon in the final products according to the following reaction (2).[23,24]

$$2Al_2O_{3(s)} + 3C_{(s)} \rightarrow Al_4O_4C_{(s)} + 2CO_{(g)} \quad (2)$$

Also, the Al_4O_4C phases could be formed through reaction between Al_2O_3 and Al_4C_3. The phase diagram calculated for the Al_2O_3–Al_4C_3 system shows that Al_4O_4C becomes stable from room temperature to 1840 °C, at which it melts eutectically.[24,25]

The SiO_2 layer on SiC and Al_2O_3 layers on Al_4SiC_4 could be efficiently removed by carbothermal reduction reactions through the incorporation of excess carbon and vacuum. In particular, the SiO_2 volume fraction in the SiC starting powder (O content of 0.45 wt%) is relatively low, and the carbothermal reduction reaction for SiO_2 removal starts to proceed at 1300 °C, which

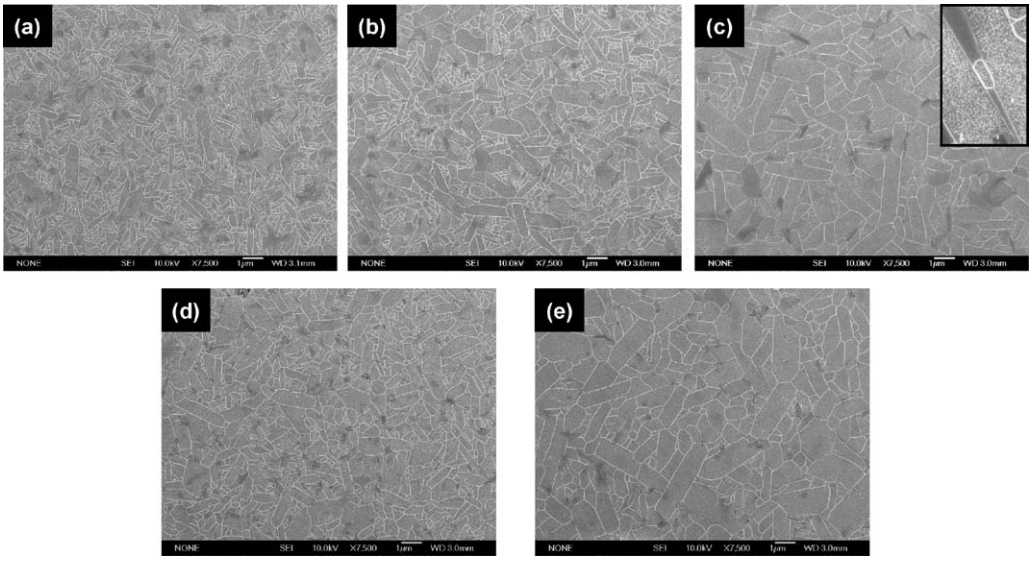

Fig. 3. SEM images for the plasma-etched surfaces of (a) ASC2, (b) ASC3, (c) ASC4, (d) ASC5, and (e) ASC6. The inset micrograph in (c) shows a highly magnified image of an identical sample which clearly indicates a trace of the liquid phase at the grain boundaries.

is 200 °C lower than that for Al_2O_3 removal.[23] Moreover, the degassing of by-product gas species from the carbothermal reaction of SiO_2 may even be easy under vacuum through a number of pore channels because SiC densification does not progress at 1300 °C.

The above discussions indicate that there is no chance of forming liquid up to 1800 °C, but liquid formation is expected to occur at 1900 °C in this study.

3.3. Densification behaviors and microstructures

Table 1 lists the relative densities of ASC1–ASC6. ASC1 showed poor sinterability but densification of SiC with a relative density of >99% was achieved when the temperature reached 1700 °C and 10 wt% additive was used. All of the SiC bulks (ASC2–ASC4) sintered with 10 wt% Al_4SiC_4 above 1700 °C showed very high sinterability. The samples with 2 and 5 wt% additive sintered at 1700 °C had low relative densities (<70%), but the densification of SiC was improved with increasing the amount of the additive.

Fig. 3 shows SEM images for the plasma-etched surfaces of ASC2–ASC6. All the specimens had nearly fully dense microstructures with elongated grains in the absence of pores. The employment of Al not only initiated densification at substantially lower temperatures, but also enhanced the β- to α-phase transformation with the growth of plate-like SiC grains.[26,27] In the samples with 10 wt% Al_4SiC_4 (ASC2–ASC4), higher temperatures led to significant grain growth but the aspect ratios of SiC grains were not dependent on temperature. The inset image in Fig. 3(c) presents a highly magnified image of ASC4, which clearly indicates a trace of the liquid phase partially existing at the grain boundaries after sintering at 1900 °C because liquid formation by the melt of Al_4O_4C occurred above 1840 °C.[25]

Larger amounts of Al_4SiC_4 additive more cause the formation of carbon particles according to the reaction (1). Generally, carbon blocks the mass transport processes which are effective in inhibiting SiC grain growth and maintaining proper dispersion of grains.[14] It was clearly observed that larger amounts of Al_4SiC_4 additive retarded more efficiently grain growth of SiC, which is certainly supported by the microstructure of ASC6 in comparison with ASC3 and ASC5. ASC6 sintered with the lowest additive content in this study had large grain size with significant grain growth due to the low carbon formation. Even though there was no clear difference on grain size in ASC3 and ASC5, however, fine grains were obviously observed in ASC3 and ASC5 with relatively high additive. This means that Al_4SiC_4 additive of 5 wt% was necessary at least in order to effectively prevent grain growth of SiC at 1800 °C by sufficient carbon formation.

3.4. Al segregation at grain boundaries

Fig. 4 shows TEM images and EDX spectra for various positions in ASC3. The EDX spectra for the grain, grain boundary, and triple junction reveal that a much larger amount of Al segregates at the grain boundary and triple junction compared to inside grains. In particular, the Al concentration at the triple junction (i.e., between three grain boundaries) is almost three times higher than at the grain boundary. The Al concentration (Fig. 4(b)) at each position was not consistent with the actual concentration in the Al_4SiC_4-doped SiC matrix, since it is very difficult to determine the exact amount of carbon at the grain boundaries by EDX or electron energy loss spectroscopy (EELS) analysis tools due to hydrocarbon contamination during TEM analysis and the very narrow grain boundary (below 1 nm). However, according to the EDX results, most of the Al resided at interfaces (grain boundary and triple junction), while a relatively small amount of Al dissolved into the SiC lattice because of its low solubility in SiC.[28] The high-resolution TEM image (Fig. 4(c)) of ASC3 definitely shows clean grain boundaries (no amorphous interlayers along the boundaries). This means

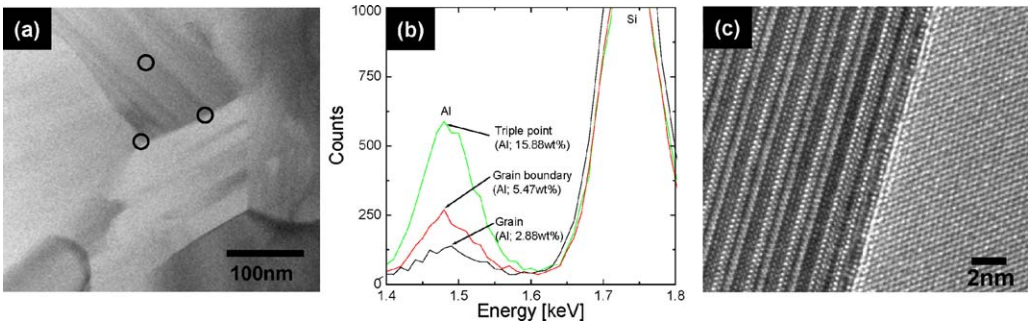

Fig. 4. (a) Typical TEM image and (b) EDX spectra for the grain, grain boundary, and triple junction regions, and (c) HR-TEM micrograph of ASC3.

that SiC densification could be obtained without the presence of a liquid phase at grain boundaries up to 1800 °C through the incorporation of Al_4SiC_4 additive in vacuum atmosphere.

SiC densification with Al_4SiC_4 doping could be achieved through the following mechanism: dissolution–reprecipitation of SiC in the melts (consequently refer to an amorphous grain boundary structure), dissolution of Al in the SiC lattice to form a solid solution, and a decrease in the interfacial energy at the grain boundaries of SiC by an activator.[29] Among the three mechanisms described above, grain boundary diffusion is believed to be the main densification mechanism in this study. The Al derived from the decomposition of the Al_4SiC_4 additive appeared to act as a sintering activator for SiC densification at low temperatures.

In order to verify the dominant mechanism for SiC densification, the densification of SiC was also carried out using 2 and 5 wt% Al_4SiC_4 additive at 1700 °C. The Al concentration of 1.17 wt% in ASC6 with the lowest additive content in this study was much higher than the solubility limit of Al in SiC (0.26 wt% at 1800 °C),[28] so the lattice diffusion by dissolution of the Al into the SiC was not limited for the formation of a solid solution. However, the densifications in both cases sintered at 1700 °C with 2 and 5 wt% additives were clearly suppressed with relative densities of lower than 70% compared to the ASC2 containing 10 wt% Al_4SiC_4. It means that the lattice diffusion is not dominant mechanism for explaining high densification of SiC at low temperature in the case of Al_4SiC_4 additive used.

Segregated Al in grain boundaries are most probably reacted with a carbon layer coated on the SiC powder to form Al_4C_3, which reaction is reported to occur at around 700 °C.[30,31] The Al-based material at the grain boundary acts as a sintering activator for SiC densification at low temperatures, accompanying to accelerate grain boundary diffusivity.[12,32] Although a small amount of Al was detected inside the SiC grain in this study, the lattice diffusion mechanism is not considered to be responsible for full densification of SiC, especially in Al heavy doping system. Consequently, a main mechanism responsible for the high densification of SiC in the SiC–Al_4SiC_4 system is believed to be induced by Al activator which was segregated at the grain boundaries. The activator most presumably modified the surface properties of grain boundaries and enhanced grain boundary diffusion.

Although the triple-junction phases were generally crystalline, their extensions into the grain boundaries do not share the same structural features, particularly in the as-prepared materials. Apparently, oxygen ions diffused from the grain boundaries to triple junctions during the high temperature processing,[33] consequently indicating the formations of Al_4C_3 phase at grain boundaries and Al_4O_4C phase at triple junctions.[34]

3.5. Fracture toughness and crack propagation

Table 1 lists the Vickers hardness (HV) and fracture toughness (K_{IC}) of ASC1–ASC6. It has commonly been accepted that hardness generally increases with decreasing grain size.[35] However, the samples sintered at different temperatures did not show a large variation in hardness values in this work because grain boundary properties of the samples were nearly identical. Specimens (ASC3, ASC5, ASC6) sintered at 1800 °C also exhibited almost the same fracture toughness values regardless of grain size (Fig. 3(b), (d), and (e)). This clearly indicates that the fracture resistance of ceramics is more dependent on grain boundary chemistry than on grain size.[5] The two fracture modes, inter- and intragranular, can be determined by the properties of the grain boundaries, which are attributed to different interfacial strengths

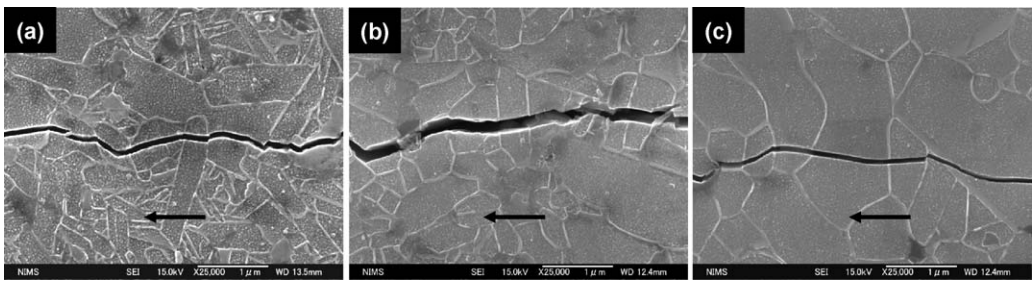

Fig. 5. SEM images for crack paths in (a) ASC3, (b) ASC5, and (c) ASC6. Arrows indicate the direction of crack propagation.

between the SiC grains. An intergranular fracture mode implies weak interfaces, whereas an intragranular facture mode indicating strong interfaces in the ceramics.[5] Fig. 5 shows SEM images for crack paths in ASC3, ASC5, and ASC6. All of the samples showed intragranular crack propagation regardless of grain size due to the strong interfacial strength between the grain and grain boundary. Intragranular crack growth behaviors in the samples indicated that grain boundary structure of Al_4SiC_4-doped SiC entirely differed from that of the ABC-SiC accompanying with a liquid phase sintering.[36]

The intragranular crack path was even observed in ASC4 with the highest toughness value by the formation of liquid phases at grain boundaries, which means that a relatively small amount of liquid phases at grain boundaries did not seem to affect the overall interfacial strength between the SiC grain and grain boundary. According to the intragranular fracture modes in this study, the beneficial effects originated from elongated grain morphology such as frictional/elastic bridging or crack deflection did not contribute to the toughening of the Al_4SiC_4-doped SiC ceramics.

4. Conclusions

The effective sintering additive Al_4SiC_4 was evaluated for both SiC densification and refinement under vacuum as a function of additive content and temperature. In the mixture of SiC and Al_4SiC_4, SiC promoted the thermal decomposition of Al_4SiC_4 due to the difference of Al content between SiC and Al_4SiC_4 grains. SiC ceramic was almost fully densified without a liquid phase at grain boundaries with 10 wt% Al_4SiC_4 additive at 1700 °C under an applied pressure of 60 MPa. Increasing the additive content efficiently retarded the grain growth of SiC due to the increasing carbon effect generated from the decomposition of the Al_4SiC_4 additive. Al activators from the additive decomposition segregated at the grain boundaries and enhanced grain boundary diffusion for SiC densification. However, SiC densification at 1900 °C was partially accompanied by liquid phase sintering originated from the melting of Al_4O_4C. All of the Al_4SiC_4-doped SiCs presented did not show the improved toughness due to the characteristics of intragranular crack propagation.

References

1. Chen D, Sixta ME, Zhang XF, Jonghe LCD, Ritchie RO. Role of the grain-boundary phase on the elevated-temperature strength, toughness, fatigue and creep resistance of silicon carbide sintered with Al, B and C. *Acta Mater* 2000;**48**:4599–608.
2. Jacobson NS. Corrosion of silicon-based ceramics in combustion environments. *J Am Ceram Soc* 1993;**76**:3–28.
3. Shinoda Y, Nagano T, Gu H. Superplasticity of silicon carbide. *J Am Ceram Soc* 1999;**82**:2916–8.
4. Mitomo M, Kim YW, Hirotsuru H. Fabrication of silicon carbide nanoceramics. *J Mater Res* 1996;**11**:1601–4.
5. Zhou Y, Hirao K, Toriyama M, Tanaka H. Silicon carbide ceramics prepared by pulse electric current sintering of β-SiC and α-SiC powders with oxide and nonoxide additives. *J Mater Res* 1999;**14**:3363–9.
6. Maître A, Put AV, Laval JP, Valette S, Trolliard G. Role of boron on the spark plasma sintering of an α-SiC powder. *J Eur Ceram Soc* 2008;**28**:1881–90.
7. Zhou Y, Tanaka H, Otani S, Bando Y. Low-temperature pressureless sintering of α-SiC with Al_4C_3–B_4C–C additions. *J Am Ceram Soc* 1999;**82**:1959–64.
8. Ray DA, Kaur S, Cutler RA, Shetty DK. Effect of additives on the activation energy for sintering of silicon carbide. *J Am Ceram Soc* 2008;**91**:1135–40.
9. Itatani K, Takahashi F, Aizawa M, Okada I, Davies IJ, Suemasu H, et al. Densification and microstructural developments during the sintering of aluminum silicon carbide. *J Mater Sci* 2002;**37**:335–42.
10. Wen GW, Huang XX. Increased high temperature strength and oxidation resistance of Al_4SiC_4 ceramics. *J Eur Ceram Soc* 2006;**26**:1281–6.
11. Lee JS, Lee SH, Nishimura T, Hirosaki N, Tanaka H. A ternary compound additive for vacuum densification of β-silicon carbide at low temperature. *J Eur Ceram Soc* 2009;**29**:3419–23.
12. Tokiyama T, Shinoda Y, Akatsu T, Wakai F. Enhancement of high-temperature deformation in fine-grained silicon carbide with Al doping. *Mater Sci Eng B* 2008;**148**:261–4.
13. Honda S, Nagano T, Kaneko K, Kodama H. Compressive deformation behavior of Al-doped β-SiC at elevated temperature. *J Eur Ceram Soc* 2002;**22**:979–85.
14. Stobierski L, Gubernat A. Sintering of silicon carbide I. *Effect Carbon Ceram Int* 2003;**29**:287–92.
15. Tanaka H, Iyi N. Simple calculation of SiC polytype contents from powder X-ray diffraction peaks. *J Ceram Soc Jpn* 1993;**101**:1313–4.
16. Anstis GR, Chantikul P, Lawn BR, Marshall DB. A critical evaluation of indentation techniques for measuring fracture toughness: I. Direct crack measurements. *J Am Ceram Soc* 1981;**64**:533–8.
17. Yang XC, Ding ZS. The synthesis and characterization of SiC nanopowder produced by chemical vapor reaction of SiH_4–C_2H_4–H_2 system. *J Mater Res* 2000;**15**:2140–4.
18. Liao T, Wang J, Zhou Y. Atomistic deformation modes and intrinsic brittleness of Al_4SiC_4: a first-principles investigation. *Phys Rev B* 2006;**74**:174112.
19. Puesche R, Hundhausen M, Ley L, Semmelroth K, Schmid F, Pensl G, et al. Study of the temperature induced polytype conversion in cubic CVD SiC by Raman spectroscopy. *J Appl Phys* 2004;**96**:5569–75.
20. Tanaka H, Hirosaki N, Nishimura T, Shin DW, Park SS. Nonequiaxial grain growth and polytype transformation of sintered α-silicon carbide and β-silicon carbide. *J Am Ceram Soc* 2003;**86**:2222–4.
21. Yoshimura HN, Cruz ACD, Zhou Y, Tanaka H. Sintering of 6H(α)–SiC and 3C(β)–SiC powders with B_4C and C additives. *J Mater Sci* 2002;**37**:1541–6.
22. Tanaka H, Zhou Y. Low temperature sintering and elongated grain growth of 6H–SiC powder with AlB_2 and C additives. *J Mater Res* 1999;**14**:518–22.
23. Lee JS, Lee SH, Nishimura T, Tanaka H. Hexagonal plate-like ternary carbide particulates synthesized by a carbothermal reduction process: processing parameters and synthesis mechanism. *J Am Ceram Soc* 2009;**92**:1030–5.
24. Qiu C, Metselaar R. Thermodynamic evaluation of the Al_2O_3–Al_4C_3 system and stability of Al-oxycarbides. *Z Metallkd* 1995;**86**:198–205.
25. Foster LM, Long G, Hunter MS. Reactions between aluminum oxide and carbon: the Al_2O_3–Al_4C_3 phase diagram. *J Am Ceram Soc* 1956;**39**:1–11.
26. Williams RM, Juterbock BN, Shinozaki S, Peters CR, Whalen TJ. Effects of sintering temperature on the physical and crystallographic properties of β-SiC. *Am Ceram Soc Bull* 1985;**64**:1385–9.
27. Shinozaki S, Williams RM, Juterbock BN, Donlon WT, Hangas J, Peters CR. Microstructural development in pressureless-sintered β-SiC materials with Al, B, and C additions. *Am Ceram Soc Bull* 1985;**64**:1389–93.
28. Tajima Y, Kingery WD. Solid solubility of aluminum and boron in silicon carbide. *J Am Ceram Soc* 1982;**65**. C-27–C-29.
29. Sameshima S, Miyano K, Hirata Y. Sinterability of SiC powder coated uniformly with Al ions. *J Mater Res* 1998;**13**:816–20.
30. Bermudez VM. Auger and electron energy loss study of the Al/SiC interface. *Appl Phys Lett* 1983;**42**:70–2.
31. Kawai C. Effect of interfacial reaction on the thermal conductivity of Al–SiC composites with SiC dispersions. *J Am Ceram Soc* 2001;**84**: 896–8.
32. Ermer E, Wieslaw P, Ludoslaw S. Influence of sintering activators on structure of silicon carbide. *Solid State Ionics* 2001;**141–142**:523–8.

33. Zhang XF, Sixta ME, Jonghe LCD. Grain boundary evolution in hot-pressed ABC-SiC. *J Am Ceram Soc* 2000;**83**:2813–20.
34. Chen D, Zhang XF, Ritchie RO. Effects of grain-boundary structure on the strength, toughness, and cyclic-fatigue properties of a monolithic silicon carbide. *J Am Ceram Soc* 2000;**83**:2079–81.
35. Rice RW, Wu CC, Borchelt F. Hardness–grain-size relations in ceramics. *J Am Ceram Soc* 1994;**77**:2539–53.
36. Yuan R, Kruzic JJ, Zhang XF, Jonghe LCD, Ritchie RO. Ambient to high-temperature fracture toughness and cyclic fatigue behavior in Al-containing silicon carbide ceramics. *Acta Mater* 2003;**51**:6477–91.